nature cell biology

Plant formin AtFH5 is an evolutionarily conserved actin nucleator involved in cytokinesis

Mathieu Ingouff[1,4,8], Jonathan N. Fitz Gerald[1,5,8], Christophe Guérin[2], Hélène Robert[1,6], Mikael Blom Sørensen[1,7], Daniel Van Damme[3], Danny Geelen[3], Laurent Blanchoin[2,9] and Frédéric Berger[1,5,9]

Formins are actin-organizing proteins that are involved in cytokinesis and cell polarity[1]. In the plant *Arabidopsis thaliana*, there are more than 20 formin homologues, all of which have unknown roles[2]. In this study, we characterize specific cellular and molecular functions of the *Arabidopsis* formin AtFH5. Despite the low identity of AtFH5 to yeast and mammalian formins, the AtFH5 protein interacts with the barbed end of actin filaments and nucleates actin-filament polymerization *in vitro*, as is the case in yeast and mammals. *In vivo*, the AtFH5–GFP fusion protein localizes to the cell plate, a plant-specific membranous component that is assembled at the plane of cell division. Consistent with these data, loss of function of *atfh5* compromises cytokinesis in the seed endosperm. Furthermore, endogenous *AtFH5* transcripts accumulate in the posterior pole of the endosperm and loss of function of *atfh5* perturbs proper morphogenesis of the endosperm posterior pole. Although cytokinesis in animals, yeast and plants occurs through morphologically distinct mechanisms, our study finds that formin recruitment to sites of actin assembly is a common feature of cell division among eukaryotes.

Formins are highly conserved proteins that are implicated in many actin-requiring processes[1], such as cytokinesis, establishment of egg polarity and formation of stress fibres. In the enhancer-trap KS117 line, the expression pattern of which provides a polarity marker for endosperm development[3], we have identified the corresponding T-DNA insertion that is localized in the upstream region of *AtFH5* and that belongs to the *Arabidopsis* formin homology (FH) family[2] (Fig. 1a). The FH2 domain of AtFH5 shares ~35% identity with other eukaryote formins and retains many highly conserved residues (see Supplementary Information, Fig. S1). By contrast, the amino terminus of AtFH5 is highly divergent from non-plant formins and shares the predicted domains that are typical of type-I *Arabidopsis* formins[2] (Fig. 1b, c). In the homologous AtFH1, this N-terminal domain is required for localization to the cell membrane[4].

In yeasts, actin patches depend on Arp2/3 complexes and cables of actin filaments depend on formins. The FH2 domain can nucleate actin filaments that grow at their barbed ends *in vitro*[5] and can control actin assembly *in vivo*[6,7]. Recent studies in *Arabidopsis* showed that extensive actin filaments can be nucleated in the absence of Arp2/3 complexes[8], indicating that a potential role may exist for formins in plants. To test whether AtFH5 nucleates actin polymerization *in vitro*, we purified two carboxy-terminal constructs of AtFH5 fused to glutathione *S*-transferase (GST) (Fig. 2a). FH1–FH2–Cter consists of FH1, FH2 and C-terminal domains, and FH2–Cter consists of the FH2 and C-terminal domains. Pyrene-labelled actin monomers were incubated alone or in the presence of FH1–FH2–Cter and assembly was monitored by pyrene fluorescence (Fig. 2b). FH1–FH2–Cter decreased the initial lag of the actin polymerization curve in a concentration-dependent manner, corresponding to active nucleation (Fig. 2b). Elongation of actin filaments nucleated by FH1–FH2–Cter with actin monomers bound to profilin confirms that these filaments are growing at their barbed ends (data not shown). The concentration of new barbed ends is strongly dependent on the presence of FH1–FH2–Cter (Fig. 2c). The curve plateaus at a high concentration of FH1–FH2–Cter because elongation of actin filaments rapidly consumes actin monomers before each formin can form new filaments (Fig. 2c). This observation is in agreement with a previous report of actin nucleation by Arp2/3 complexes[9]. Filament length is inversely correlated to the concentration of nucleation centres. Accordingly, actin filaments are markedly shorter in the presence of FH1–FH2–Cter (mean length, 5.3 ±5 μm) (Fig. 2e) than alone (mean length, 18 ±17 μm) (Fig. 2d).

[1]EMBO YIP team, Unité Mixte de Recherche 5667, Institut Fédératif de Recherche 128 BioSciences Lyon-Gerland, Ecole Normale Supérieure de Lyon, 46 allée d'Italie, F-69364 Lyon cedex 07, France. [2]Laboratoire de Physiologie Cellulaire Végétale, Commissariat à l'Energie Atomique, Centre National de la Recherche Scientifique, Université Joseph Fourier, 17 rue des martyrs, F-38054 Grenoble, France. [3]Department of Plant Systems Biology, VIB-Ghent University, Technologiepark 927, B-9052 Gent, Belgium. [4]Present address: Laboratoire de Physiologie Cellulaire Végétale, Commissariat à l'Energie Atomique, Centre National de la Recherche Scientifique, Université Joseph Fourier, 17 rue des martyrs, F-38054 Grenoble, France. [5]Present address: Temasek Lifesciences Laboratory, 1 Research Link, National University of Singapore, Singapore 117604. [6]Present address: Institute of Biology of Leiden, Clusius Laboratory, Wassenaarseweg 64, AL 2333 Leiden, The Netherlands. [7]Present address: Plant Research Department, PRD-301, Risø National Laboratory, PO Box 49, DK-4000 Roskilde, Denmark. [8]These authors contributed equally to this work.
[9]Correspondence should be addressed to F.B. (e-mail: fred@tll.org.sg) or L.B. (e-mail: laurent.blanchoin@cea.fr)

Published online: 13 March 2005; DOI: 10.1038/ncb1238

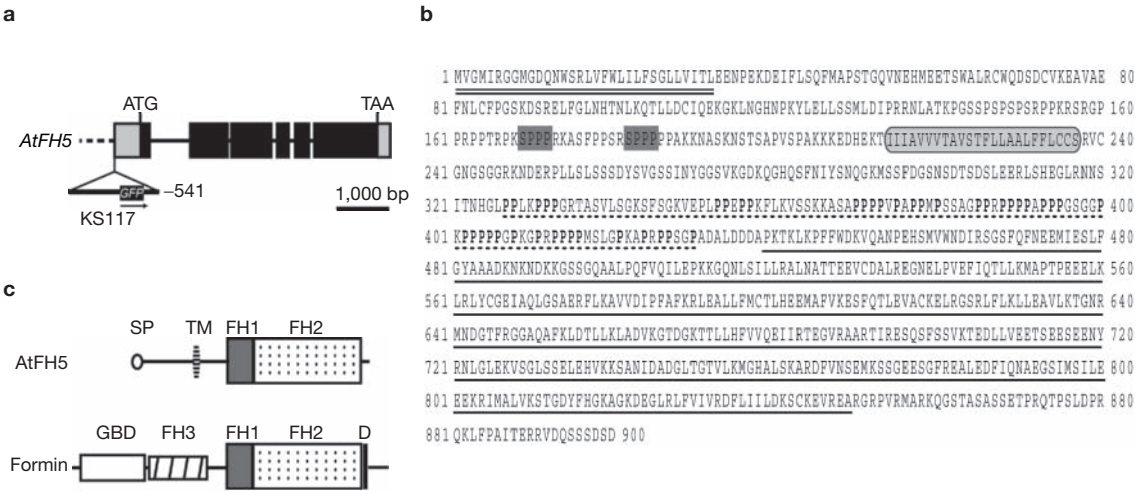

Figure 1 *AtFH5* encodes a formin protein. (**a**) Schematic drawing of the *AtFH5* locus. The T-DNA insertion in the KS117 enhancer-trap green fluorescent protein (GFP) line is localized 541 base pairs upstream of the putative translation (ATG) start site. Exons and introns are represented by black boxes and lines, respectively, and the *AtFH5* upstream region is represented by a dotted line. The 5′- and 3′-untranslated regions are boxed in grey. (**b**) Predicted domains of the putative AtFH5 formin protein. The amino-terminus of AtFH5 has a putative signal peptide (double line) followed by a repeated SPPP motif (shaded) and a predicted transmembrane domain (circled in grey). The AtFH5 protein features the two typical carboxy-terminal domains of formins: the formin homology 1 (FH1) domain (dotted line), which is rich in proline (in bold), and the formin homology 2 (FH2) domain (underlined). (**c**) Domain organization in AtFH5 and other non-plant formins. The typical domains encountered in non-plant formins are depicted. Apart from the FH1–FH2 unit, AtFH5 shows no homology with the identified targeting (FH3) or regulatory domains (**d**, GBD) of formin. Note that formin domains are not drawn to scale. D, diaphanous autoregulatory domain; FH1, formin homology 1; FH2, formin homology 2; FH3, formin homology 3; GBD, Rho-GTPase binding domain; SP, signal peptide; TM, transmembrane domain.

To initially ascertain barbed-end dynamics in the presence of AtFH5, a constant concentration of actin filaments was incubated with increasing concentrations of FH1–FH2–Cter before the addition of labelled actin monomers (Fig. 2f). The initial rate of elongation, which is proportional to the number of available free actin-filament barbed ends, decreased as we increased the FH1–FH2–Cter concentration. This indicates that the barbed ends of preformed filaments were capped with high affinity (K_d ~32 nM) by pre-incubation with FH1–FH2–Cter (Fig. 2f). In addition, pyrene-labelled actin filaments were diluted below the barbed-end critical concentration (0.1 μM) in the presence of increasing amounts of FH1–FH2–Cter (Fig. 2g). The initial rate of depolymerization decreased with increased FH1–FH2–Cter concentration, again in agreement with a barbed-end capping activity. Interestingly, the FH2–Cter protein has no effect on actin nucleation (Fig. 2h). However, FH2–Cter inhibits the actin nucleation that is driven by FH1–FH2–Cter, indicating that FH2–Cter competes with FH1–FH2–Cter for binding actin monomers.

The biochemical analysis of AtFH5 indicates that the actin-organizing activity of formins is conserved throughout eukaryotes. To determine if such nucleating activity could also be related to cytokinesis, we examined AtFH5 subcellular localization in roots in which *AtFH5* is expressed in the wild type. AtFH5 was tagged with green fluorescent protein (GFP) and expressed in transgenic *Arabidopsis* plants. We used the constitutive CaMV 35S promoter that enables dynamic observations in roots, with enhanced optical resolution in comparison to that seen in endosperm. Fluorescence microscopy showed that AtFH5–GFP fluorescence accumulates in the cell plate of dividing root cells (Fig. 3). The AtFH5–GFP signal follows the expanding plate over time and its intensity gradually reduces after contact is made between the cell plate and the parent cell wall. The dynamic localization of AtFH5 protein to the cell plate indicates that AtFH5 has a role in cytokinesis. A fluorescent dotted pattern of undetermined identity was also observed in the cytoplasm (Fig. 3) and might not reflect the true localization of AtFH5, as potential artifacts may be associated with overexpression of AtFH5–GFP.

The endosperm in the *Arabidopsis* plant seed provides a simple and tractable system for studying cytokinesis within a multinucleate single cell[10]. Endosperm development involves a series of successive nuclear divisions that are devoid of cytokinesis, generating a syncytium[11,12]. After eight rounds of division, the syncytium contains approximately 200 nuclei that become partitioned into mononucleate cells by a cytokinetic mechanism that is referred to as cellularization[12]. Cellularization initiates from the anterior pole, where the embryo develops, and continues towards peripheral endosperm, ending at the posterior pole that remains syncytial[11,13]. Nuclei at this pole are included in large multinucleate structures called nodules that gradually migrate and eventually fuse with the cyst at the most posterior location[14].

As the GFP activity in the AtFH5-tagged KS117 line indicated a role for this gene in endosperm development[3], we examined the *AtFH5* expression pattern during seed development. *AtFH5* mRNAs were localized in the endosperm by *in situ* hybridization on seed sections. A strong expression was specific to the posterior pole in the cyst (Fig. 4a) and in nodules on top of the cyst (Fig. 4a, inset). No expression was detectable in the anterior and peripheral endosperm or in other seed compartments (such as the embryo and the seed coat). Expression of *AtFH5* was further confirmed in transgenic *Arabidopsis* expressing the nuclear fluorescent reporter Histone2B–Yellow Fluorescent Protein (H2B–YFP) under the control of the *AtFH5* upstream region. H2B–YFP is first detected in the posterior endosperm early in development (Fig. 4c) and remains restricted to the posterior pole (Fig. 4d) throughout the syncytial phase.

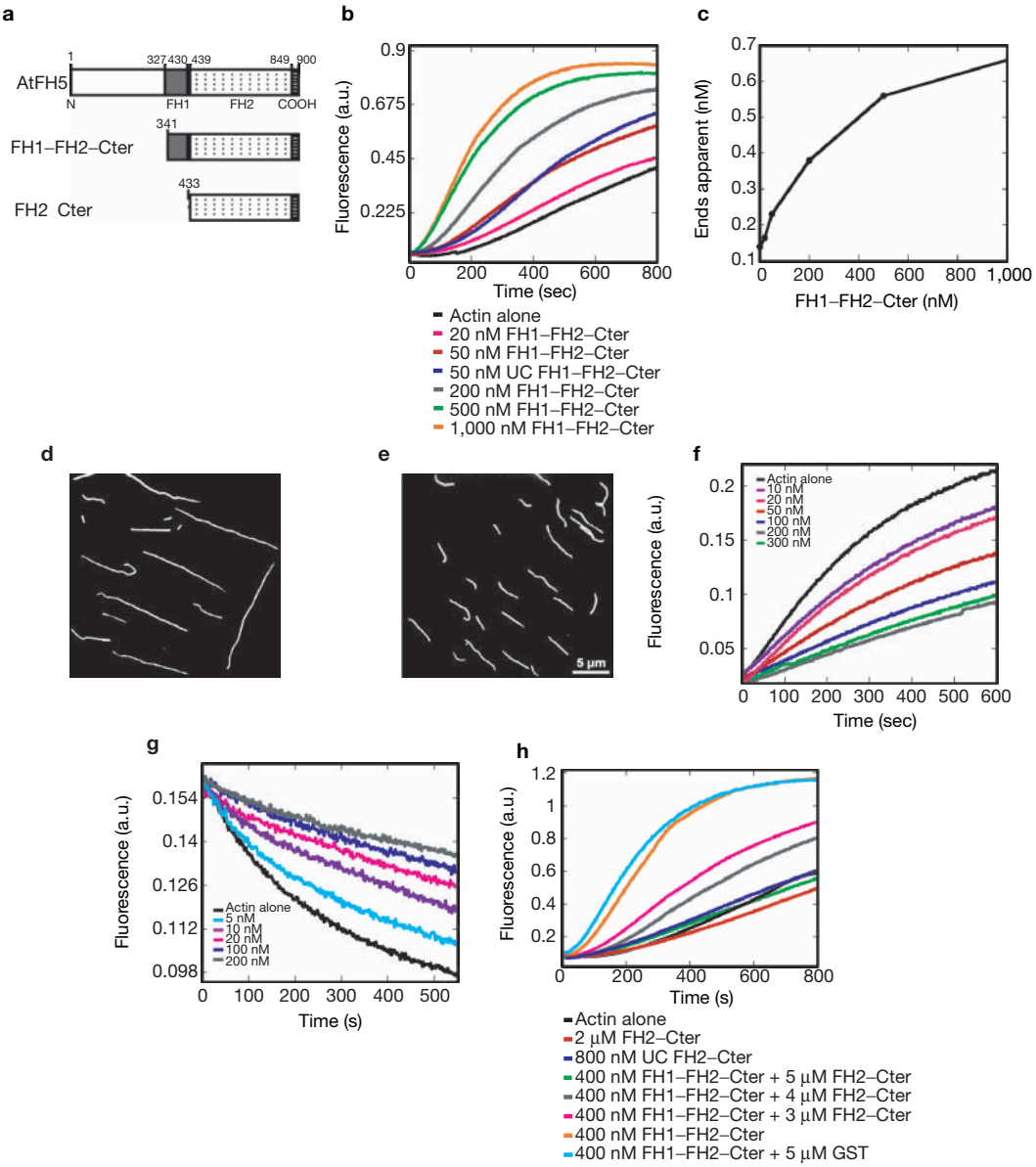

Figure 2 AtFH5 (FH1–FH2–Cter) nucleates and caps actin filaments *in vitro*. (**a**) Schematic representation of domain organization of AtFH5, FH1–FH2–Cter and FH2–Cter constructs. (**b**) Actin (4 µM, 10% pyrene-labelled) was assembled in the presence of the indicated concentrations of the FH1–FH2–Cter protein. (**c**) The apparent concentration of barbed ends, as previously reported[9]. (**d,e**) Fluorescence micrographs of the products of actin polymerization. (**d**) Mg–ATP–actin alone; (**e**) 500 nM FH1–FH2–Cter. (**f**) Kinetics of the elongation of actin-filament barbed ends in the presence of the indicated concentrations of FH1–FH2–Cter protein. (**g**) Kinetics of depolymerization of actin-filament barbed ends in the presence of the indicated concentrations of FH1–FH2–Cter protein. (**h**) Actin (4 µM, 10% pyrene-labelled) was assembled in the presence of the indicated concentrations of FH2–Cter and/or FH1–FH2–Cter proteins. UC symbol represents unfrozen glutathione *S*-transferase (GST)-cleaved proteins. All others proteins were used as GST-tagged proteins.

This pattern persists after endosperm cellularization (Fig. 4e). Together, these two experiments indicate that *AtFH5* expression is restricted to the posterior pole throughout endosperm development. However, GFP was also detected in the anterior and peripheral syncytial endosperm in the KS117 line[3], indicating that the enhancer activity detected by KS117 GFP does not entirely mimic the endogenous *AtFH5* pattern.

To gain insight into *AtFH5* function during endosperm development, we examined two *atfh5* insertional mutant lines (Fig. 5a, top). Reverse transcription PCR (RT-PCR) expression analyses with primers downstream of the insertions revealed no *AtFH5* transcripts (Fig. 5a, bottom). A barely detectable level of *AtFH5* transcripts was obtained with primers that were positioned upstream of the insertions. These *atfh5* mutations probably result in loss of function as neither of the two mutants expresses the actin-organizing domains of AtFH5. Although *AtFH5* is expressed in most tissues, we could not detect any phenotypes in vegetative organs, probably due to the redundant function with other formins. Microscopic examination of *atfh5;atfh5* seeds revealed perturbation of endosperm cellularization. Cleared siliques were used to score the onset of cellularization in wild-type and *atfh5* mutant lines (Fig. 5b). Whereas most wild-type endosperm is cellularized by the heart

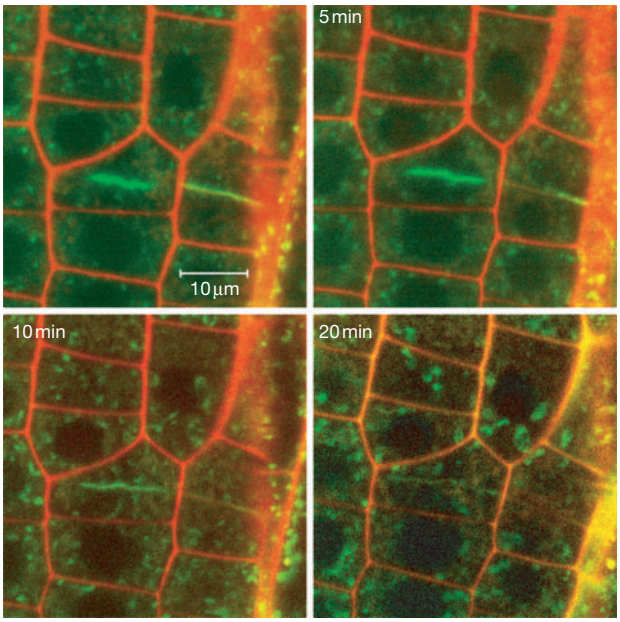

Figure 3 Formin AtFH5–GFP is targeted to the developing cell plate. Time series of a confocal section of the cortical layer near the tip of an *Arabidopsis* root expressing AtFH5–GFP. AtFH5–GFP fluorescence was concentrated in cells undergoing cytokinesis, and accumulated in young and maturing cell plates. Fluorescence was strongly reduced in cell walls that were just completed. In the cytoplasm, fluorescent dot-like organelles were observed. The contours of the root cells were prestained with propidium iodide for 10 min (red signal). Scale bar, 10 µm; time points are indicated in min.

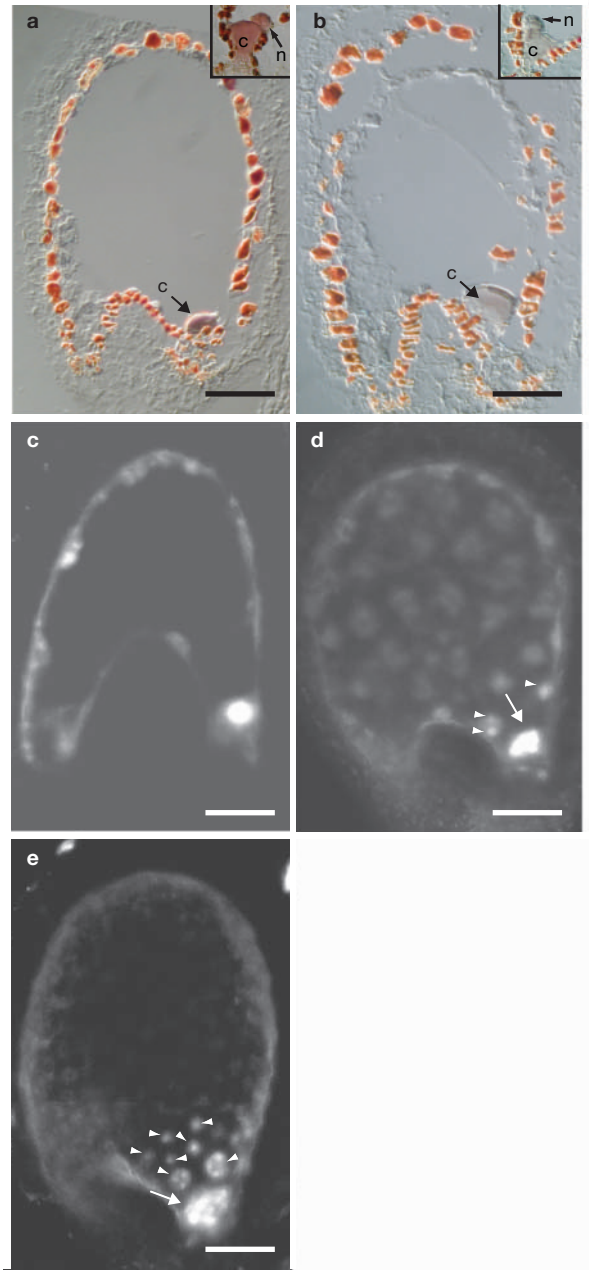

Figure 4 *AtFH5* expression is restricted to the posterior pole during endosperm development. (**a–b**) *In situ* hybridization of *AtFH5* transcripts in the endosperm. Sections hybridized with an antisense (**a**) or sense (**b**) *AtFH5* probe. *AtFH5* mRNAs are specifically detected in the cyst (arrow) and in the nodules (see inset **a**) of posterior endosperm in the sections that had been hybridized with the antisense probe. Scale bars, 40 µm. (**c–e**) *AtFH5::H2B–YFP* expression in the endosperm analysed by confocal laser microscopy. H2B–YFP fusion protein is first detected in one nucleus of posterior endosperm at the 16-nuclei stage (**c**), and becomes localized in the cyst consisting of multiple nuclei (arrow) and mono- and binucleate nodules (arrowheads) at the 48-nuclei stage (**d**). By the heart-embryo stage, H2B–YFP activity remains in mono- and multi-nucleate nodules and in the cyst (**e**). Scale bars, 20 µm for **c**; 30 µm for **d**; 40 µm for **e**. c, cyst; n, nodule.

embryo stage, cellularization was delayed at that embryo stage in *atfh5* endosperm. Nevertheless, cellularization occurred in the endosperm of both mutant alleles later — during the late heart embryo stage when wild-type endosperm is completely cellularized. To ascertain the origin of the delay of cellularization in *atfh5* endosperm, we compared the onset of cellularization between wild-type and *atfh5* endosperm. In the wild-type endosperm, cellularization occurs after nuclei division and is initially marked by a cell plate between separating sister nuclei[13]. This is rarely seen in fixed tissue (circa 0.02%; $n > 5{,}000$), as complete cellularization is rapidly achieved by the formation of cell plates between non-sister nuclei (Fig. 5c, d; also see Supplementary Information, Fig. S2). In contrast to the wild type, this early cellularization step was frequently observed in *atfh5* endosperm (a few seeds per silique at appropriate stages; $n > 500$), indicating a delay of this cytokinetic process (Fig. 5g; also see Supplementary Information, Figs S2,S3a, b). This would indicate that the time required for cell-plate formation and maturation is prolonged without wild-type *AtFH5*. Accordingly, binucleate cells were detected in *atfh5-2* endosperm (see Supplementary Information, Fig. S2). As *AtFH5* transcripts seem to be confined to the posterior pole, the effects of *atfh5* mutations on cellularization in other parts of the endosperm could be explained if AtFH5 protein is translocated from the posterior pole towards the other domains of the endosperm.

In addition to defective cellularization, *atfh5* mutations perturb the ontogenesis of the cyst at the endosperm posterior pole (Fig. 5f, h; also see Supplementary Information, Fig. S3c). At the embryo heart stage in the wild-type endosperm, cyst formation was evident in most seeds, with only 8.1% of seeds ($n = 62$) containing a weakly discernible cyst (Fig. 5c, e). However, a complete absence of cyst structure was observed in 18.8% of the *atfh5-1* seeds ($n = 64$), although nodules were consistently apparent around the site at which a cyst would normally form (Fig. 5f, h).

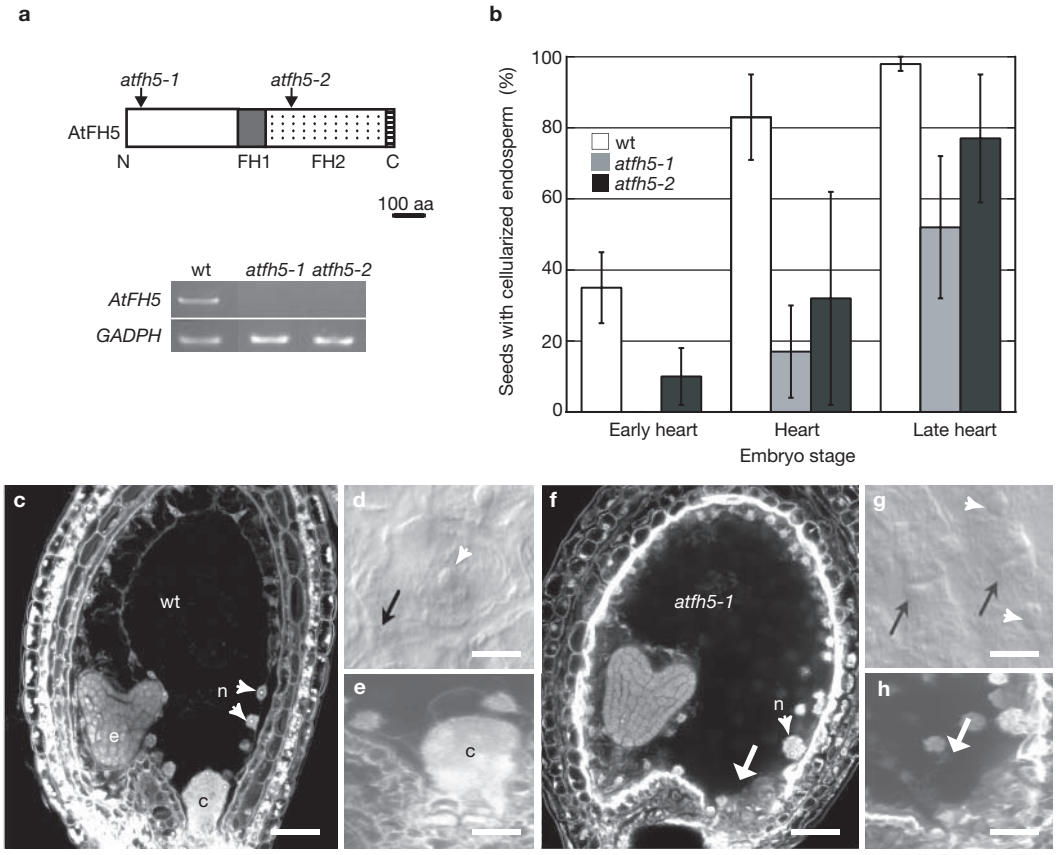

Figure 5 Molecular characterization of the *AtFH5* locus. (**a**) Structure of the putative *AtFH5* formin. The T-DNA insertion site in *atfh5* mutant alleles is indicated by an arrow. Expression of *AtFH5* was analysed by real-time PCR in siliques from wild-type (wt) and *atfh5;atfh5* mutants. *GADPH* is the PCR control. (**b**) Delayed endosperm cellularization in *atfh5;atfh5* mutants. Cleared siliques were used to score the onset of cellularization in wild-type and *atfh5* lines with differential interference contrast microscopy. Wild-type (n=269; 97 heart embryo stages), *atfh5-1* (n=206; 68 heart embryo stages) and *atfh5-2* (n=178; 79 heart embryo stages) seeds were scored for embryo stage and the presence of visible cellularized endosperm. Percentages represent percent of embryo class, per plant, that were completely cellularized. (**c–e**) Wild-type endosperm development. (**c**) At the heart embryo stage, the endosperm cellularization is initiated at the anterior pole around the embryo (**e**) and progresses toward the posterior pole where a cyst (**c**) and nodules (n, see arrows) on top of the cyst differentiate. (**d**) Cellularization is easily distinguished by the double cell-wall layer (black arrow) surrounding the nuclei (white arrowhead). (**e**) Enlarged view of the cyst (c). (**f–h**) *atfh5-1* endosperm development. (**f**) In *atfh5-1*, seed endosperm cellularization is slightly delayed and differentiation of structures in the posterior endosperm is affected. (**g**) Cellularizing cells with cell plates (black arrows) crossing between sister nuclei (white arrowheads). (**h**) At the posterior pole, nodules are formed but the cyst, normally resulting from oriented migration of nodules, is absent. Scale bars, 50 μm for **c**, **f**; 20 μm for **d**, **g**; 50 μm for **e**, **h**.

A similar reduction of cyst was observed in *atfh5-2* endosperm (see Supplementary Information, Fig. S3c). Cyst formation requires directional migration of nuclei towards the basal posterior endosperm to generate the cyst[14]. The cytoskeletal tracks that are required for directional nuclei movement could involve either the microtubule or actin-based network, as both kind of cytoskeleton are present at the posterior pole in an *Arabidopsis* relative[15]. We hypothesize that AtFH5 acts on the dynamics of specialized cytoskeletons, thereby enabling local nuclei migration towards the cyst. We attempted dynamic visualization of actin cytoskeleton in the wild-type endosperm, with the GFP fused to the actin-binding domain of mouse talin protein[16] under the control of the *ACTIN11* promoter[17]. This generated diffuse patterns of fluorescence in the posterior pole. This may be due to insufficient optical resolution or to artefacts generated by GFP–Talin[16]. No labelling was detected in other parts of the endosperm. Dynamic localization of AtFH5 will be necessary to further understand the role of formin during endosperm development.

We find that *Arabidopsis* type-I formin AtFH5 has biochemical activity that is similar to yeast and mammalian formins[5]. *In vitro* purified FH1–FH2–Cter fragments of AtFH5 nucleate actin filaments that grow at their barbed ends. Surprisingly, in contrast to mammalian[18] and yeast formins[19,20], this activity is not supported by the FH2–Cter fragment of AtFH5 alone, indicating that FH1 domain and the few amino acids between the FH1 and FH2 domains are necessary for nucleating activity.

Cytokinesis in plants has been thought to involve mostly microtubule-dependent structures and vesicular transport[21,22], in contrast to animal cytokinesis in which actin and contractile forces have a major role[23]. However, during plant cytokinesis, short actin filaments are assembled *de novo* at the cell plate[24,25]. The role of actin in this compartment is unclear, but microinjection of profilin, a formin-interacting protein, delays or completely inhibits cell-plate formation[26], and actin-depolymerizing drugs affect cell-plate guidance[27,28]. Based on AtFH5 localization and its biochemical properties, these short actin filaments would be assembled

through a formin-dependent mechanism that is not exclusive to AtFH5, as *atfh5* loss of function shows a delayed cytokinesis in endosperm and not in vegetative tissues.

In endosperm, *atfh5* loss of function partially affects cytokinesis and morphogenesis. The eventual cellularization and formation of a cyst at the posterior endosperm in *atfh5* mutants could be attributed to functional redundancy with other related formins[2]. In the *atfh5* mutants, cell-plate expansion between sister and non-sister nuclei was conspicuously stalled during cellularization, indicating that *AtFH5* is required for completion of cytokinesis. Subcellular localization of AtFH5–GFP to the incipient and expanding cell plate in roots further supports a role in cell-plate maturation. Similar to *atfh5* mutants, completion of the cell plate during cytokinesis is delayed in plant cells that overexpress phragmoplastin[29]. Phragmoplastin is a dynamin-like protein that is associated with membranous vesicle fusion at the cell plate[29]. One hypothesis to explore is that newly polymerized short actin filaments at the cell plate would participate in fine-tuning vesicle trafficking and fusion, enabling optimized membrane reconstitution as the cell plate expands.

Our study highlights the importance of actin and associated regulators, including formins, for the completion of higher-plant cytokinesis (as is the case in animals). It therefore becomes probable that, together with microtubules and vesicle trafficking, actin filaments participate in higher-plant and animal cytokinesis but use distinct scaffolds. □

METHODS

Plant material and growth conditions. The KS117 (C24 accession) line was identified in the Jim Haseloff's enhancer-trap GFP line collection (http://www.plantsci.cam.ac.uk/Haseloff). The *atfh5-1* (Ws accession, FST 542F06) and *atfh5-2* (Columbia accession, SALK_044464) mutants were obtained from the T-DNA mutant collections of INRA Versailles and the SALK institute, respectively. Plants were grown as reported previously[14].

Cloning of *AtFH5*. Sequences of flanking regions of the KS117 (C24 accession) line were identified and used to determine the position of the T-DNA insertion by homology searches against the *Arabidopsis thaliana* (Columbia accession) genome (http://www.arabidopsis.org/). The KS117 insertion is located in the upstream region of the *At5g65540* gene. The corresponding gene in the C24 accession was amplified by PCR and entirely sequenced; it features the same exon–intron structure.

Biochemical methods. Two deleted *AtFH5* fragments — FH1–FH2–Cter and FH2–Cter — were amplified by PCR from a RAFL clone containing *AtFH5* cDNA (pda02156; RIKEN BioResource Center, Japan) using *Sal*I-R (5′-TTAGTCTG AATCTGAACTAGACTGATCCACG-3′) with *Sal*I-FH1 (5′-AGGTCGACG ATCAGGGAAGTCTTTTTCTGGA-3′) or *Sal*I-FH2 (5′-AGGTCGACGATT AGATGATGATGCTCCCAAAA-3′) primers. Error-free *Sal*I-PCR fragments were ligated to a pGEX-4T1 vector (Promega, Charbonnieres, France) that was linearized by a *Sal*I restriction enzyme. These constructs were overexpressed in the RosettaBlue (DE3)pLysS strain of *Escherichia coli* (Novagen, Madison, WI). Cultures were resuspended in extraction buffer (25 mM Tris (pH 7.5), 500 mM NaCl, 5% glycerol, 0.1% Triton X-100, 1 mM EDTA and 1 mM dithiothreitol), with protease inhibitor cocktail. After sonication and centrifugation (at 23,000 *g* for 30 min), supernatants were incubated with gluthatione-sepharose 4B (Amersham, Piscataway, NJ), washed with TBSE (25 mM Tris (pH 7.5), 500 mM NaCl, 1 mM EDTA and 1 mM dithiothreitol) and eluted with 100 mM glutathione in TBSE or cleaved with thrombin before elution with TBSE. Eluted proteins were dialysed against storage buffer (25 mM Tris (pH 8.0), 50 mM KCl, 1 mM EDTA, 1 mM dithiothreitol and 1 mM azide) and concentrated with Centriprep YM-30 (Amicon, Bedford, MA) and used directly or flash frozen in liquid nitrogen.

Fluorescence assay for actin polymerization or depolymerization. Actin (10% pyrene-labelled) was polymerized by the addition of 1:9 dilution of 10x KMEI (500 mM KCl, 10 mM $MgCl_2$, 10 mM EGTA and 100 mM imidazole at pH 7.0). Actin polymerization in the presence of AtFH5 purified proteins was followed by changes in pyrene fluorescence (excitation at 365 nm and emission at 407 nm) using a MOS450 Bio-Logic fluorimeter (Bio-Logic-Science Instruments SA, Claix, France) or a Xenius SAFAS (Safas SA, Monaco). Elongation or depolymerization assays to follow the capping activity of purified AtFH5 constructs have been described previously[30]. Both purified FH1–FH2–Cter and FH2–Cter proteins lacking the GST tag showed properties similar to those of GST–FH1–FH2–Cter and GST–FH2–Cter, indicating that the GST tag does not contribute to any of the tested activities (Fig. 2b, h). All purified proteins were tested before or after freezing with no change in activities (Fig. 2b, h).

Plasmid construction and transformation. PCR reactions were performed with the Expand High Fidelity kit (Roche Diagnostics, Brussels, Belgium). All the promoter fusion (*AtFH5::H2B–YFP*) and protein fusion (*35S::AtFH5–EGFP*) constructs were generated with the Gateway cloning technology (Invitrogen, Carlsbad, CA). Primers with *att*B1 and *att*B2 sequences were purchased from Invitrogen. Details of plasmids can be found in Supplementary Methods. *Arabidopsis* plants were transformed using the *Agrobacterium*-mediated floral dip method[31]. Primary seed transformants were selectively grown on MS medium supplemented with kanamycin (50 μg ml^{-1}).

Characterization of *atfh5* mutant alleles. Expression of *AtFH5* in both mutant lines was analysed by RT-PCR. Briefly, total RNA was extracted from siliques using RNeasy kit (Qiagen, Hilden, Germany). cDNA was produced with oligo(dT) primer and SuperScript II reverse transcriptase (Invitrogen). One-tenth of each cDNA sample was added to PCR reactions using primers F-FH52F (5′-AACAATCATTAGCACCAACTCTTC-3′) and R-FH52R (5′-ATTGCCGATTCTACAGCTTTTTG-3′) to amplify the 5′untranslated region of the *AtFH5* transcript, and FH5F2754 (5′-GTGCAAGCAAACCCAG AACATTCAATGGT-3′) and FH5R3074 (5′-GTCTGAATCTGAACTAGACTG ATCCACG-3′) to amplify the 3′ untranslated region of the *AtFH5* transcript.

Microscopy. Fluorescence of H2B–YFP and AtFH5–GFP protein fusions was analysed using confocal laser scanning microscopy on a LSM-510 CLSM or an inverted Axiovert Zeiss 100 M microscope (Zeiss, Jena, Germany).

Seeds of transgenic F2 lines for *AtFH5::H2B–YFP* constructs were analysed with the GFP excitation setting. The two valves of siliques were removed and lines of seeds still connected to the septum were freshly mounted in Murashige and Skoog culture medium (Sigma, Saint-Quentin Fallavier, France) supplemented with 0.3% (w/v) plant agar (Duchefa, The Netherlands). For each construct, H2B–YFP activity showed similar expression patterns. Seedlings (F2 generation) overexpressing *AtFH5–GFP* were imaged with excitation settings (488 nm for GFP, 543 nm for propidium iodide 2 d after germination.

The images were captured with the LSM510 image acquisition software (Zeiss). Digital image processing was performed with Photoshop 7 and Illustrator 9 (Adobe Systems, San Jose, CA).

Actin filaments were observed *in vitro* by epifluorescence illumination, as previously reported[9], with a Zeiss-Axioplan microscope. Digital images were collected with a Hamamatsu ORCA charge-coupled camera using Axiovision software (Zeiss).

To study the phenotype of endosperm in *atfh5* mutants, seeds were fixed and analysed by confocal microscopy as described previously[3].

To quantify the delay in endosperm cellularization of *atfh5* mutants, seeds at selected stages of embryo development — ranging from the early heart to the torpedo stage — were dissected from individual siliques and cleared in Hoyer's medium[12]. The phenotype was analysed by microscopy using differential interference contrast (DIC) optics (Optiphot, Nikon, Japan) coupled with a AxioCam MRc digital camera (Zeiss). Images were processed with Axiovision software (Zeiss).

***In situ* hybridization.** Seeds were fixed overnight in 4% paraformaldehyde. The tissues were dehydrated by means of a graded series of ethanol and embedded in Paraplast Plus (Sigma).

Two PCR products containing T7 polymerase promoter in either orientation were obtained with T7-F2754 (5′-T7-TGCAAGCAAACCCAGAACATTCA ATGG-3′) and R3384 (5′-CAAAAGCCATTTCTTCATGGAGTGTACACA-3′) or F2754 and T7-R3384 primers. The sense and antisense RNA probes were

synthesized from purified PCR fragments with incorporation of digoxigenin (DIG RNA Labelling Kit, Roche Biochemicals, Brussels, Belgium).

The prehybridization, hybridization and washes were performed as described previously[32]. The hybridization signals were analysed with a Nikon (Tokyo, Japan) microscope using DIC optics.

Accession numbers. The GenBank accession number of At5g54650 (C24 accession) is Y581683.

Note: Supplementary Information is available on the Nature Cell Biology website.

ACKNOWLEDGEMENTS

We gratefully acknowledge the Institut National de la Recherche Agronomique Versailles and the SALK Institute for providing the insertion mutant lines; and the RIKEN Bioresource Center for prodiving the *AtFH5* full-length cDNA clones. We thank C. Dumas for hosting F. B.'s team in his Reproduction et Développement des Plantes laboratory (Lyon, France). We thank A. Chaboud and S. Corneille for sharing Gateway plasmid constructs and S. Madi for valuable technical advice. We thank F.-Y. Bouget for his help in setting up a screen to identify phragmoplast-localized GFP-tagged proteins. This work was supported by the French Génoplante II programme (M.I.). The work was sponsored by the International Research Fellowship Program of the National Science Foundation (Grant INT 0301886; J.FG.), by the Fund for Scientific Research-Flanders (D.G. and D.V.D.), by a Marie Curie postdoctoral fellowship from the European Commission (M.B.S.), by the Institut National de la Recherche Agronomique (F.B., J.FG.) and by ATIPE from the Centre National de la Recherche Scientifique (C.G. and L.B.). F.B. is part of the European Molecular Biology Organisation Young Investigator Program. We thank D. Kovar, H. Higgs and T. Pollard for helpful suggestions.

COMPETING FINANCIAL INTERESTS

The authors declare that they have no competing financial interests.

Received 4 January 2005; accepted 15 January 2005
Published online at http://www.nature.com/naturecellbiology

1. Evangelista, M., Zigmond, S. & Boone, C. Formins: signaling effectors for assembly and polarization of actin filaments. *J. Cell Sci.* **116,** 2603–2611 (2003).
2. Deeks, M.J., Hussey, P.J. & Davies, B. Formins: intermediates in signal-transduction cascades that affect cytoskeletal reorganization. *Trends Plant Sci.* **7,** 492–498 (2002).
3. Sørensen, M.B., Chaudhury, A.M., Robert, H., Bancharel, E. & Berger, F. Polycomb group genes control pattern formation in plant seed. *Curr. Biol.* **11,** 277–281 (2001).
4. Cheung, A.Y. & Wu, H.M. Overexpression of an *Arabidopsis* formin stimulates supernumerary actin cable formation from pollen tube cell membrane. *Plant Cell* **16,** 257–269 (2004).
5. Zigmond, S.H. Formin-induced nucleation of actin filaments. *Curr. Opin. Cell Biol.* **16,** 1–7 (2004).
6. Evangelista, M., Pruyne, D., Amberg, D.C., Boone, C. & Bretscher, A. Formins direct Arp2/3-independent actin filament assembly to polarize cell growth in yeast. *Nature Cell Biol.* **4,** 32–41 (2002).
7. Kovar, D.R., Kuhn, J.R., Tichy, A.L. & Pollard, T.D. The fission yeast cytokinesis formin Cdc12p is a barbed end actin filament capping protein gated by profilin. *J. Cell Biol.* **161,** 875–887 (2003).
8. Deeks, M.J. & Hussey, P.J. Arp2/3 and 'the shape of things to come'. *Curr. Opin. Plant Biol.* **6,** 561–567 (2003).
9. Blanchoin, L. *et al.* Direct observation of dendritic actin filament networks nucleated by Arp2/3 complex and WASp/Scar proteins. *Nature* **404,** 1007–1011 (2000).
10. Berger, F. Endosperm: the crossroad of seed development. *Curr. Opin. Plant Biol.* **6,** 42–50 (2003).
11. Brown, R.C., Lemmon, B.E., Nguyen, H. & Olsen, O.A. Development of endosperm in *Arabidopsis thaliana*. *Sex Plant Reprod.* **12,** 32–42 (1999).
12. Boisnard-Lorig, C. *et al.* Dynamic analyses of the expression of the HISTONE::YFP fusion protein in *Arabidopsis* show that syncytial endosperm is divided in mitotic domains. *Plant Cell* **13,** 495–509 (2001).
13. Sørensen, M.B. *et al.* Cellularisation in the endosperm of *Arabidopsis thaliana* is coupled to mitosis and shares multiple components with cytokinesis. *Development* **129,** 5567–5576 (2002).
14. Guitton, A.E. *et al.* Identification of new members of Fertilisation Independent Seed Polycomb Group pathway involved in the control of seed development in *Arabidopsis thaliana*. *Development* **131,** 2971–2981 (2004).
15. Nguyen, H., Brown, R.C. & Lemmon, B.E. Patterns of cytoskeletal organization reflect distinct developmental domains in endosperm of *Coronopus didymus* (Brassicaceae). *Intl J. Plant Sci.* **162,** 1–14 (2001).
16. Ketelaar, T., Anthony, R.G. & Hussey, P.J. Green fluorescent protein-mTalin causes defects in actin organization and cell expansion in *Arabidopsis* and inhibits actin depolymerizing factor's actin depolymerizing activity *in vitro*. *Plant Physiol.* **136,** 3990–3998 (2004).
17. Huang, S., An, Y.Q., McDowell, J.M., McKinney, E.C. & Meagher, R.B. The *Arabidopsis ACT11* actin gene is strongly expressed in tissues of the emerging inflorescence, pollen, and developing ovules. *Plant Mol. Biol.* **33,** 125–139 (1997).
18. Shimada, A. *et al.* The core FH2 domain of diaphanous-related formins is an elongated actin binding protein that inhibits polymerization. *Mol. Cell* **13,** 511–522 (2004).
19. Pruyne, D. *et al.* Role of formins in actin assembly: nucleation and barbed-end association. *Science* **297,** 612–615 (2002).
20. Xu, Y. *et al.* Crystal structures of a Formin Homology-2 domain reveal a tethered dimer architecture. *Cell* **116,** 711–723 (2004).
21. Verma, D.P. Cytokinesis and building of the cell plate in plants. *Annu. Rev. Plant Physiol. Plant Mol. Biol.* **52,** 751–784 (2001).
22. Mayer, U. & Jürgens, G. Microtubule cytoskeleton: a track record. *Curr. Opin. Plant Biol.* **5,** 494–501 (2002).
23. Robinson, D.N. & Spudich, J.A. Mechanics and regulation of cytokinesis. *Curr. Opin. Cell Biol.* **16,** 182–188 (2004).
24. Staehelin, L.A. & Hepler, P.K. Cytokinesis in higher plants. *Cell* **84,** 821–824 (1996).
25. Endle, M.C., Stoppin, V., Lambert, A.M. & Schmit, A.C. The growing cell plate of higher plants is a site of both actin assembly and vinculin-like antigen recruitment. *Eur. J. Cell Biol.* **77,** 10–18 (1998).
26. Valster, A.H., Pierson, E.S., Valenta, R., Hepler, P.K. & Emons, A. Probing the plant actin cytoskeleton during cytokinesis and interphase by profilin microinjection. *Plant Cell* **9,** 1815–1824 (1997).
27. Palevitz, B. & Hepler, P.K. The control of the plane of division during stomatal differentiation in *Allium*. II. Drug studies. *Chromosoma* **46,** 327–341 (1974).
28. Schmit, A.C. & Lambert, A.M. Characterization and dynamics of cytoplasmic F-actin in higher plant endosperm cells during interphase, mitosis, and cytokinesis. *J. Cell Biol.* **105,** 2157–2166 (1987).
29. Gu, X. & Verma, D.P. Dynamics of phragmoplastin in living cells during cell plate formation and uncoupling of cell elongation from the plane of cell division. *Plant Cell* **9,** 157–169 (1997).
30. Huang, S., Blanchoin, L., Kovar, D.R. & Staiger, C.J. Arabidopsis capping protein (AtCP) is a heterodimer that regulates assembly at the barbed ends of actin filaments. *J. Biol. Chem.* **278,** 44832–44842 (2003).
31. Clough, S.J. & Bent, A.F. Floral dip: a simplified method for *Agrobacterium*-mediated transformation of *Arabidopsis thaliana*. *Plant J.* **16,** 735–743 (1998).
32. Jackson, D. *Plant Pathology, Vol I: A Practical Approach* (eds Gurr, S.J., McPherson, M.J. & Bowles, D.J.) 163–174 (IRL Press, Oxford, 1992).

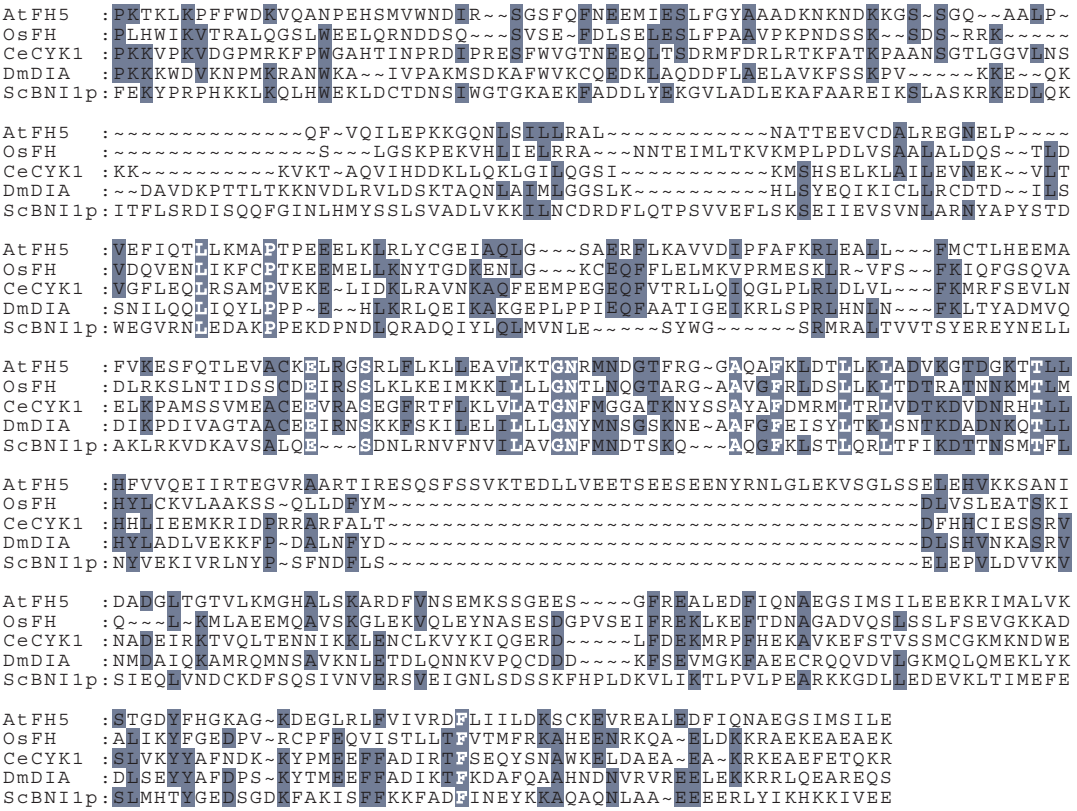

Figure S1 Sequence alignment of the FH2 domain in formins from highly divergent organisms. The crystallised FH2 domain from *S. cerevisiae* Bni1p formin is as a reference for the alignment[1]. Identical residues are shaded in grey when found in at least three of the five proteins. The residues conserved among all sequences are marked in white. Accession numbers (Acc. Num.): *A. thaliana* Formin Homology 5 (AtFH5, Acc. Num. AY581683; *C. elegans* cytokinesis defect-1 (CeCYK-1, Acc. Num. NP_741211); *D. melanogaster* diaphanous (DmDia, Acc. Num. P48608); *O. sativa* predicted formin homology protein (OsFH, Acc. Num. BAC55695); *S. cerevisiae* bud neck involved 1 (ScBni1p, Acc. Num. NC_14128).

1. Xu, Y. *et al.* Crystal structures of a Formin Homology-2 domain reveal a tethered dimer architecture. *Cell* **116,** 711–723 (2004).

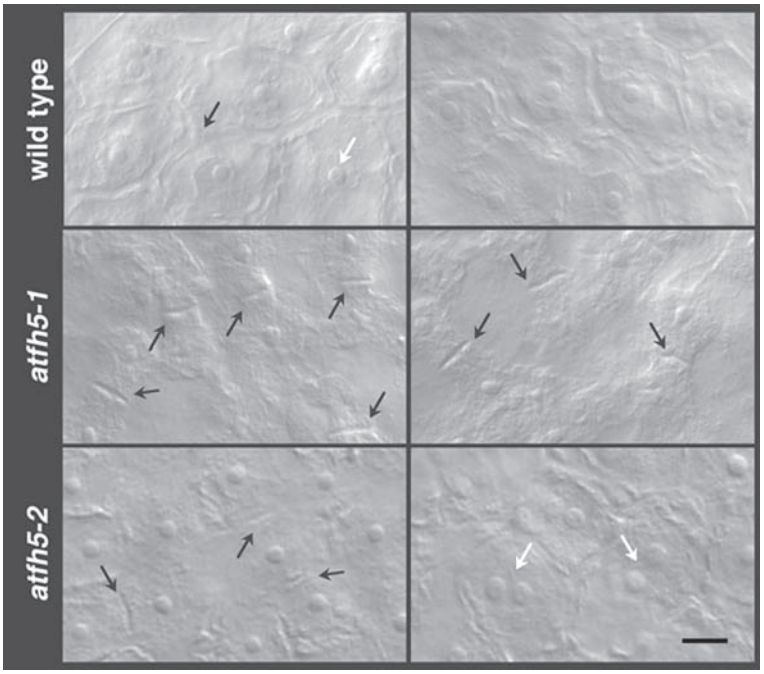

Figure S2 Delayed cellularisation in *atfh5* mutant alleles. DIC images of cleared heart stage embryo seeds from wild type and *atfh5* plants were taken to illustrate the cellularisation defects in these mutant alleles. In wild type (top panels), cellularisation is demonstrated by the double lines in regular polygonal patterns (black arrow) around a single nucleus (white arrow). The *atfh5-1*/*atfh5-1* mutant (middle panels) at the same stage was notable for the incomplete cellularisation and the occurrence of single walls (black arrow) between nuclei. The *atfh5-2*/*atfh5-2* mutant also features this phenotype (black arrows, left bottom panel). Further, in some of the *atfh5-2* seeds where cellularisation occurred, binucleate cells were observed (white arrows, right bottom panel). Scale bar represents 20 µm.

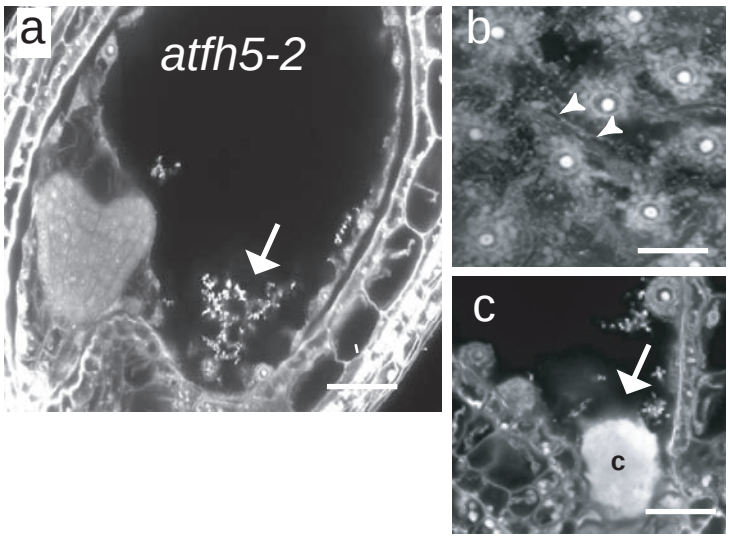

Figure S3 Abnormal endosperm development in *atfh5-2* mutant allele. (a) Confocal sections of *atfh5-2* seeds showing a slight delay of endosperm and reduction of cyst size in the posterior endosperm. (b) As in *atfh5-1* cellularising cells appear with cell plates crossing between sister nuclei (white arrows). (c) At the posterior pole, nodules are formed but the cyst (c) can be reduced in size compared to wild type. Scale bars represent 50 µm for a; 20 µm for b; 50 µm for c.

SUPPLEMENTARY METHODS

Plasmid construction. PCR reactions were performed with the Expand High Fidelity kit (Roche Diagnostics, Brussels, Belgium). All the final constructs were generated with the Gateway((cloning technology (Invitrogen, Carlsbad, CA). Primers with *att*B1 and *att*B2 sequences were purchased from Invitrogen.

AtFH5::H2B-YFP constructs. Two fragments of the upstream region of *AtFH5* were amplified by PCR with *att*B1-P1 (5'-*att*B1-gagagaaattgacgaatga-3') and *att*B2-R1 (5'-*att*B2-ATCTTTTGCTTCTCATTTCATCAG-3') or *att*B1-P3 (5'-*att*B1-AAGGTCCGATGCCTAATGGA-3') and *att*B2-R1 (5'-*att*B2-ATCTTTTGCTTCTCATTTCATCAG-3'). Both PCR products contain the 5'-UTR (460 bp long) and 1840 bp of the putative promoter region for the P1-R1 fragment (long FH5 construct, FH5L) and 850 bp of the putative promoter region for the P3-R1 fragment (short FH5 construct, FH5S). The pDONR207-FH5L and pDONR207-FH5S entry vectors were obtained by BP reaction cloning (Invitrogen).

The cassette Histone2B-Yellow Fluorescent Protein and the nopaline synthase terminator (H2B-YFP-nos) was amplified from pBI121-35S::H2B-YFP-nos vector[1] with primers H2B-YFP (5'-GGGCCCGGGATGGCGAAGGCAGATAAGAAAC-3') and nos (5'-CCCGGGCCATGCCTACAGGTCACTGGAT-3') containing respectively *Sma*I and *Apa*I restriction sites at their 5' end. The *Sma*I/*Apa*I H2B-YFP-nos fragment was cloned into the *Sma*I/*Apa*I sites of the binary vector pGREEN-NII (pGII) (http://www.pGREEN.ac.uk/; ref. 2). The Gateway recombination cassette with reading frame B (rfB) was inserted into *Sma*I site of pGII-H2B-YFP-nos to generate the "destination vector" pGII-rfB-H2B-YFP-nos. Recombination reactions (*att*L x *att*R) were performed between the "destination vector" pGII-rfA-H2B-YFP-nos and either the pDONR207-FH5L or pDONR207-FH5S entry vectors to produce respectively the vectors pGII-FH5L::H2B-YFP and pGII-FH5S::H2B-YFP.

Spatial and temporal expression pattern of H2B-YFP in transgenic Arabidopsis plants containing pGII-FH5L::H2B-YFP or pGII-FH5S::H2B-YFP was identical.

35S::AtFH5-GFP construct

To construct a GFP-tagged version of the formin *AtFH5* (*At5g54650*) putative start and stop codons were used to design the forward primer (5'-ATGGTTGGAATGATTCGAGGAGG-3') and the reverse primer (5'- GTCTGAATCTGAACTAGACTGATCCACG-3') to which *att*B1 and *att*B2 extensions for Gateway® (Invitrogen, Carlsbad, CA) were added. The stop codon was replaced by a tyrosine codon for in-frame cloning with the Enhanced Green Fluorescent Protein (EGFP). cDNA was cloned from poly(A+) RNA extracted from *Arabidopsis* suspension cells following a one step RT-PCR reaction (Titan one tube RT-PCR kit; Roche Diagnostics, Brussels, Belgium) with high-fidelity DNA polymerase. PCR products were gel-purified (High pure PCR purification kit; Roche Diagnostics), and subcloned into pDONR207 via BP reaction cloning. The AtFH5 insert was transferred to the pK7WGF2 "destination vector"[3] to generate EGFP C-terminal fusions downstream of the strong constitutive CaMV 35S promoter.

1. Boisnard-Lorig, C. *et al*. Dynamic analyses of the expression of the HISTONE::YFP fusion protein in Arabidopsis show that syncytial endosperm is divided in mitotic domains. *Plant Cell* **13,** 495–509 (2001).
2. Hellens, R. P., Edwards, E. A., Leyland, N. R., Bean, S. & Mullineaux, P. M. pGreen: a versatile and flexible binary Ti vector for Agrobacterium-mediated plant transformation. *Plant Mol. Biol.* **42,** 819–832 (2000).
3. Karimi, M., Inze, D. & Depicker, A. GATEWAY vectors for Agrobacterium-mediated plant transformation. *Trends Plant Sci.* **7,** 193–195 (2002).